Breaking the Limitation of Evanescent Wave Sensing with Subwavelength Grating Waveguides

Hai Yan[1,4], Lijun Huang[1,2,4], Xiaochuan Xu[3,4], Swapnajit Chakravarty[3], Naimei Tang[3], Huiping Tian[2], and Ray T. Chen[1,3]

[1]*Department of Electrical and Computer Engineering, The University of Texas at Austin, Austin, TX 78758, USA*
[2]*State Key Laboratory of Information Photonics and Optical Communications, School of Information and Communication Engineering, Beijing University of Posts and Telecommunications, Beijing 100876, China*
[3]*Omega Optics Inc., 8500 Shoal Creek Blvd., Austin, TX, 78759, USA*
[4]*These authors contributed equally to this paper.*
Email address: raychen@uts.cc.utexas.edu

Abstract: Microring resonator based on subwavelength grating waveguides was studied and demonstrated in biosensing experiment to show its thickness-independent high sensitivity, which breaks the limitation in conventional evanescent wave sensors.
OCIS codes: (280.4788) Optical sensing and sensors; (130.3120) Integrated optics devices; (050.6624) Subwavelength structures

On-chip photonic biosensors can potentially achieve high sensitivity, high throughput, and label-free detection [1]. Various devices, including surface plasmon devices, microring resonators, silicon nanowires, photonic crystal (PC) microcavities, have been demonstrated [2]. Most of the sensors are based on the interaction between the evanescent wave and the biomolecules immobilized on the sensor surface. The sensitivity drops inevitably with increasing thickness of the surface layer accumulated on the sensor surface, which is the intrinsic limitation of evanescent wave based sensors. Here we analyzed and demonstrated unique thickness-independent surface sensitivity in microring resonator biosensor based on recently proposed subwavelength grating (SWG) waveguides [3]. The SWG waveguide consists of periodic silicon pillars with a period much smaller than the operating wavelength. In the SWG waveguides, effective sensing region includes not only the top and side of the waveguide, where evanescent wave exists, but more importantly the space between silicon pillars on the light propagation path. The surface sensitivity remains constantly high even when surface layer thickness grows.

The structure of the SWG microring resonator is shown in Fig. 1(a) and (b). It is constructed by replacing the strip waveguides in a conventional microring resonator with SWG waveguides [3]. The silicon SWG microring resonator sits on top of the buried oxide layer and is covered by the sensing medium (water or other biological buffers). The SWG in the microring resonator uses trapezoidal pillars to minimize bending loss and achieve better quality factors [4]. The SWG in the bus waveguide still uses regular rectangular pillars. The radius of the microring R is set to 10μm. The grating period of the SWG is Λ=200 nm. Duty cycle of the grating (ratio of silicon pillar length l to grating period Λ) η=0.65 and waveguide width w = 450 nm are chosen to achieve overlapping factor σ = 0.4. The top and bottom bases (a and b) of the trapezoidal pillars are optimized to 100 nm and 150 nm, respectively.

The simulated electric field intensity distribution is shown in Fig.1(c) (top view) and (d) (front view). It can be seen that in contrast to the evanescent field on the top surface and sidewalls of the waveguide, there is significantly stronger field existing on the light propagation path between silicon pillars. In resonance based sensing method, surface sensitivity S_s can be defined as the resonance wavelength shift in according to the change of surface layer thickness [3]: $S_s = \Delta\lambda/\Delta t = (\lambda / n_g)(\partial n_{eff} / \partial t)$, where n_g is group index and t is the thickness of surface layer. We

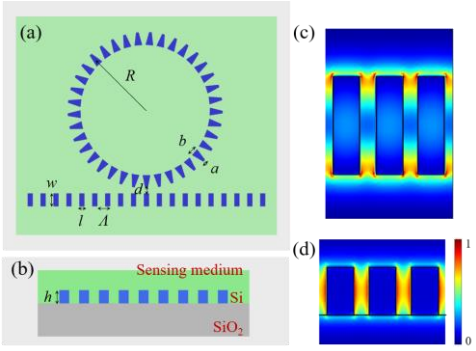

Fig. 1. Top view (a) and front view (b) of the SWG microring structure; Top view (c) and front view (d) of the electric field intensity distribution.

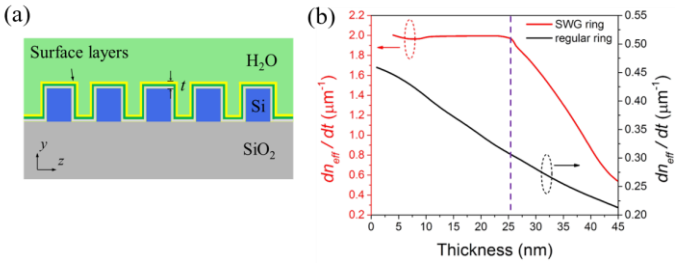

Fig. 2. (a) (a) Schematic of the SWG structure covered by thin layers of silicon dioxide, chemicals and immobilized protein in water environment; (b) Comparing dn_{eff}/dt as the thickness of surface layer grows in SWG microring and conventional microring.

compared $\partial n_{eff} / \partial t$ in both SWG and conventional waveguide in simulation. We assume the sensing medium is water (n = 1.32) and the surface layer has uniform thickness across the surface with uniform refractive index of n = 1.48 [3]. The simulation results are shown in Fig. 2(b). The $\partial n_{eff} / \partial t$ in SWG waveguide is 4-6 times larger than that in a regular strip waveguide due to large mode overlapping factor. Furthermore, the value remains constantly high in SWG structure for the first 25nm of the surface layer, while in strip waveguide, $\partial n_{eff} / \partial t$ drop monotonically with the accumulation of surface layers. This result coincides with the above mode profile analysis and shows that SWG structure has superior ability to maintain high surface sensitivity when the thickness of surface layer grows.

The SWG microring resonator was fabricated and the bulk refractive index sensitivity of the SWG microring biosensor was first characterized with different concentrations of glycerol-water solutions. The results in Fig. 3(a) shows a bulk sensitivity of 440.5 ± 4.2 nm/RIU, which is several times higher than that of a conventional microring resonator [5]. Then the SWG microring resonator went through a biosensing test side by side with a conventional microring resonator on the same chip. The chip surface was first treated with (3-Aminopropyl) triethoxysilane (APTES) and glutaraldehyde (GLU) to create a layer that can immobilize protein covalently. Next, anti-streptavidin antibody (anti-SA, 50 μg/mL), bovine serum albumin (BSA, 1 mg/mL), streptavidin (SA, 100 μg/mL), and biotinylated BSA (bio-BSA, 1 mg/mL) were flowed in sequence into the microfluidic channel containing both microring sensors for interactions. BSA was used as blocking buffer. Before switching reagent at each of the above steps, phosphate buffer saline (PBS) buffer was flowed to remove any unbound biomolecules. Resonance wavelengths of both the SWG and conventional microring were recorded and resonance shifts were compared.

The resonance shifts for both microring biosensors are shown in Fig. 3(b). Resonance shift in SWG microring are 4-6 times larger than that in regular microring as expected. It can also be seen that as more and more layers built on the surface, the resonance shift difference between the two microrings also becomes larger. To explicitly show this difference, surface sensitivity with respect to the thickness of surface layer is compared in Fig. 3(c). The thickness of the surface layers is estimated by combining the simulated surface sensitivity and the experimental resonance shift in SWG microring. The surface sensitivity of the SWG ring is $S_s \approx 1.0 nm/nm$ (λ = 1550 nm, n_g = 3.0, assume n = 1.48 across all surface layer) for the first 25 nm thick of surface layer. Therefore, the surface layer thickness can be estimated ($\Delta t = \Delta\lambda / S_s$). The surface sensitivity of the regular microring can then be calculated by $S_s = \Delta\lambda / \Delta t$. Figure 3(c) shows that the sensitivity of the microring resonator drops monotonically compared to that of the SWG ring as thickness of accumulated biomolecules grows continuously. It is worth noting that both devices were tested side by side in the same microfluidic channel, the surface layer thickness can be taken as the same, thus the resonance shift at each thickness can be compared. The estimated thickness in the x-axis of Fig. 3(c) also takes into account the initial thickness of silicon dioxide (~5 nm) and APTES (~5nm).

In conclusion, we have shown that the limitation of surface layer thickness in evanescent wave sensors can be overcome by the use of SWG waveguides in which the sensitivity remains constantly high when thickness grows.

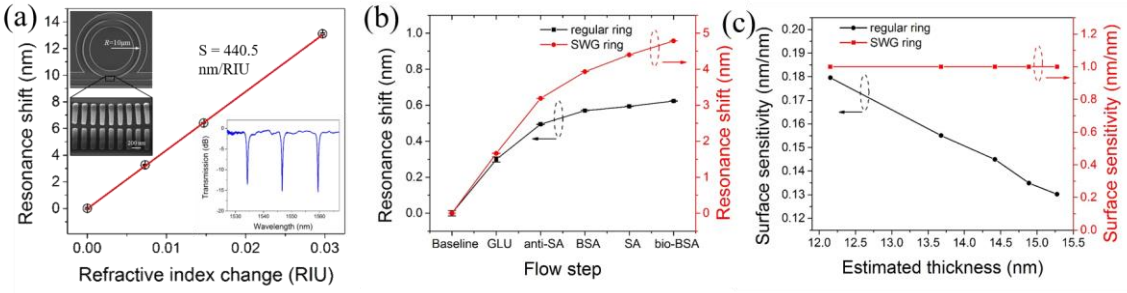

Fig. 3. (a) Resonance shift with respect to refractive index change. Insets show SEM image of the SWG microring resonator and its transmission spectrum; (b) Resonance shift in both SWG microring and regular microring; (c) Surface sensitivity with respect to estimated thickness in both SWG microring and regular microring.

This research was supported by the US Department of Energy (DOE) (Contract #: DE SC-0013178) and National Cancer Institute/ National Institutes of Health (NCI/NIH) (Contract #: HHSN261201500039C).

References

[1] M. C. C. Estevez, et al., Integrated optical devices for lab-on-a-chip biosensing applications, Laser Photon. Rev. **6**, 463–487 (2012).
[2] V. Passaro, et al., Recent Advances in Integrated Photonic Sensors, Sensors **12**, 15558–15598 (2012).
[3] J. Flueckiger, et al., Sub-wavelength grating for enhanced ring resonator biosensor," Opt. Express **24**, 15672 (2016).
[4] Z. Wang, et al. , Geometrical tuning art for entirely subwavelength grating waveguide based integrated photonics circuits, Sci. Rep. **6**, 24106 (2016).
[5] M. Iqbal, et al., Label-Free Biosensor Arrays Based on Silicon Ring Resonators and High-Speed Optical Scanning Instrumentation, IEEE J. Sel. Top. Quantum Electron. **16**, 654–661 (2010).